CrossMark

An Improved Structured Low-Rank Representation for Disjoint Subspace Segmentation

Lai Wei[1] (iD) **· Yan Zhang[1] · Jun Yin[1] · Rigui Zhou[1] · Changming Zhu[1] · Xiafeng Zhang[1]**

Abstract

Low-rank representation (LRR) and its extensions have shown prominent performances in subspace segmentation tasks. Among these algorithms, structured-constrained low-rank representation (SCLRR) is proved to be superior to classical LRR because of its usage of structure information of data sets. Compared with LRR, in the objective function of SCLRR, an additional constraint term is added to compel the obtained coefficient matrices to reveal the subspace structures of data sets more precisely. However, it is very difficult to determine the best value for the corresponding parameter of the constraint term, and an improper value will decrease the performance of SCLRR sharply. For the sake of alleviating the problem in SCLRR, in this paper, we proposed an improved structured low-rank representation (ISLRR). Our proposed method introduces the structure information of data sets into the equality constraint term of LRR. Hence, ISLRR avoids the adjustment of the extra parameter. Experiments conducted on some benchmark databases showed that the proposed algorithm was superior to the related algorithms.

Keywords Subspace segmentation · Spectral clustering · Low-rank representation · Structure constraint

---

✉ Lai Wei
  weilai@shmtu.edu.cn

  Yan Zhang
  smuzhangyan@163.com

  Jun Yin
  junyin@shmtu.edu.cn

  Rigui Zhou
  rigui@shmtu.edu.cn

  Changming Zhu
  cmzhu@shmtu.edu.cn

  Xiafeng Zhang
  xfzhang@shmtu.edu.cn

[1] Department of Computer Science, Shanghai Maritime University, Haigang Avenue 1550, Shanghai, China

1 Introduction

In recent years, subspace segmentation has played an important role in image representation, computer vision, and other related fields [1–5]. The ultimate aim of subspace segmentation is to classify data samples to their corresponding subspaces. According to the surveys in related research works [6–8], major treatment methods for subspace segmentation include algebraic methods [9, 10], iterative methods [11, 12], statistical methods [13, 14], and spectral clustering-based methods [6–8, 15–21]. Among them, the methods based on spectral clustering have achieved great successes in practical applications.

Generally speaking, a spectral clustering based subspace segmentation algorithm consists of two steps: (1) constructing an affinity matrix for a given data set; (2) obtaining the final segmentation result via a special spectral clustering algorithm (e.g. Ncut [22]) with the constructed affinity matrix. It can be observed that the obtained affinity matrix usually determines the performance of a spectral clustering based subspace segmentation algorithm.

The existing methods for learning affinity matrices could all be regarded as self-representation models. The principal ideology of a self-representation model is that each sample data can be linearly represented by the other data samples from the same data set. For that, Elhamifar and Vidal [15, 20] first proposed a sparse subspace clustering (SSC) algorithm, which aims to calculate a reconstruction coefficient vector by l_1-minimization [23] for each data sample and then construct a sparse affinity matrix by concentrating all the reconstruction coefficient vectors. SSC is designed to obtain the sparsest representation of each sample, but the global structures of data sets are usually ignored. To capture the global structures of grossly corrupted data sets, Liu et al. [7, 18] developed a low-rank representation algorithm (LRR) to discover the reconstruction coefficients matrix for all data points jointly. LRR expects the coefficient matrix to have a minimal rank, and this goal can be satisfied by minimizing its nuclear norm. It's proved that the minimal nuclear norm constraint would make the coefficient matrix is capable of discovering the global structure of corrupted data points. Therefore, LRR performs better than SSC in corrupted subspace segmentation problems.

In addition, a lot of approaches have been proposed to show the capabilities of low-rank methods in different applications [24–29]. Wang et al. [24] developed a novel DCT (discrete cosine transform) regularized low-rank method to handle image recovery problems for data with large percentage of corruption. In [25], for solving matrix completion problems, Hu et al. used a kind of truncated nuclear norm, which is gotten by the nuclear norm subtracted by the sum of the largest few singular values, to replace the classical nuclear norm. To accelerate the convergence of the TNNR, Liu et al. presented a TNNR-WRE algorithm, in which different weights were given to the corresponding rows of the residual error matrix [26]. Wang et al. formulated a new robust PCA algorithm to discover the low-rank and noisy components simultaneously [27]. Li et al. [28] proposed a discriminative multi-view interactive image re-ranking algorithm which could describe the images sufficiently by integrating user relevance feedback capturing users' intentions and multiple features. Li et al. [29] proposed an efficient image retrieval algorithm, called SPA (Spatially Pooled Attributes for image retrieval), which encoded weak spatial information into attribute embedding.

The wide usages in image applications of LRR and its successes in constructing affinity graphs have encouraged lots of related subsequent researches. For example, Chen et al. [30] considered a symmetric low-rank representation to preserve the high-dimensional data sets' subspace structure. Zhuang et al. [31] presented the locality-preserving low-rank representation to obtain an undirected graph from a mixture of nonlinear manifolds. Zhang et al.

Fig. 1 The sensitivity of SCLRR to parameter β when λ is fixed, λ is the parameter to the residual term
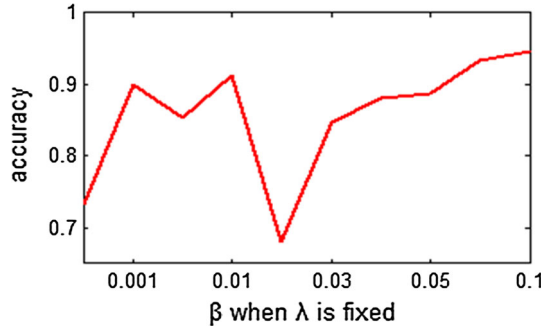
[32] claimed that the structured low-rank representation of a data matrix could be learned by using a supervised method to create a discriminant and reconstructive dictionary. Zhuang et al. introduced a non-negative low rank and sparse representation (NNLRSR) method [33] by adding non-negative and sparse constraints of the reconstruction coefficient matrix into LRR. Experiments showed that these algorithms can get promising results in subspace segmentation for different data sets.

However, the original LRR algorithm can only work well under the condition that the subspaces of a data set are totally independent. Therefore, Tang et al. [34] raised a structure-constrained low-rank representation (SCLRR) to handle disjoint subspace segmentation problems. SCLRR incorporates the structure information of data sets by appending a regularization term in the objective function of LRR, which is a feasible approach for solving multiple disjoint subspace segmentation problems. On the basis of SCLRR, Li et al. [35] advanced a structure-constrained low-rank dictionary learning (SCLRDL) algorithm to combine low-rank constraint with structure information into coefficient matrix for image classification. Wu et al. [36] overcome the shortcomings of existing techniques in handling disjoint subspaces and proposed a CS-LRR algorithm to perform optimal spectral clustering of the subspaces. To find the optimal low-rank affinity matrices of disjoint data sets for Ncut, Wei et al. proposed a SCSLRR algorithm [8] to combine the objection functions of K-means, Ncut, and LRR together.

For SCLRR, its appended regularization term brings an additional parameter into LRR and different values of the parameter have great effect on the efficiency of the algorithm. Furthermore, there is already a parameter for the residual term in the original LRR algorithm, hence SCLRR has been a more complex double parameters problem. In Fig. 1, we give a simple experiment on Fashion-MINIST [37] data set to observe the sensitivity of SCLRR to the additional regularization parameter β, it can be seen that the performance of SCLRR varies drastically with β.

Therefore, we attempt to find a better way to introduce the structure information of data sets into LRR and solve the disjoint subspace segmentation problems. In this paper, a new improved structured low-rank representation algorithm, abbreviated as ISLRR, is presented. In ISLRR, we introduce the structure information of data sets into the equality constraint term of LRR. It can be found that ISLRR evades the difficulty of tuning two parameters. Experiments on some benchmark data sets demonstrate that ISLRR is easy to implement and efficient for disjoint subspace segmentation tasks.

The main framework of this article is as follows: In Sect. 2, we briefly introduce LRR and SCLRR. In Sect. 3, we give the motivation of ISLRR and present an optimization algorithm to solve ISLRR. In Sect. 4, we give some further discussions about the proposed algorithm.

Experiments for verifying the effectiveness of our algorithm are shown in Sect. 5. Finally, Conclusions are presented in Sect. 6.

2 Related Algorithms

In this section, we briefly describe LRR and its extended algorithm SCLRR.

2.1 Low-Rank Representation

Suppose a data matrix $X = [x_1, x_2, \ldots, x_n] \in \mathbb{R}^{d \times n}$, where d is the dimensions of each data sample and n is the number of all samples. Because each data sample can be lineally represented by the data samples from the same subspace, the model can be written as:

$$X = AZ, \tag{1}$$

where $A = [a_1, a_2, \ldots, a_m] \in \mathbb{R}^{d \times m}$ is a dictionary and Z is the reconstruction coefficient matrix. In LRR, X is used as the dictionary and Z is hoped to have minimal rank. Then the purpose of LRR can be expressed as:

$$\min_Z rank(Z) \text{ s.t. } X = XZ. \tag{2}$$

However, in real-world applications, data points are usually noisy and even grossly corrupted. So the objective function of LRR can be rewritten as:

$$\min_{Z,E} \|Z\|_* + \lambda \|E\|_{2,1} \text{ s.t. } X = XZ + E, \tag{3}$$

where $\|E\|_{2,1} = \sum_{i=1}^{n} \sqrt{\sum_{j=1}^{n} \left([E]_{ij}\right)^2}$ ($[E]_{ij}$ is the (i,j)-th element of E) is called $l_{2,1}$-norm of noise E and $\lambda > 0$ is a parameter to balance the contributions of two parts.

Augmented Lagrange multipliers (ALM) [18] method can be used to solve the problem (3). Once Z is obtained, we can define $G = \left(Z + Z^T\right)/2$ (Z^T is the transpose of Z) as the affinity graph and use Ncut [22] to get the final clustering results.

2.2 Structure-Constrained Low-Rank Representation

As we know, LRR algorithm can only work well on data sets with independent subspaces. Independent subspaces segmentation is a special case of the disjoint subspace segmentation. To improve the capability of LRR for handling disjoint subspace segmentation problems, SCLRR adds a weighted sparse matrix $|M \odot Z|_1 = \sum_{i,j} M_{ij} |Z|_{i,j}$ (M is a matrix which characterizes the locality structure information of a data set) into the objective function to enhance the structure information of Z. For that, the penalty of rank is weaker than that in the objective function which only considers the nuclear norm, therefore, the structure constraint can also improve the rank of the solution. As the above descriptions, considering the noise and outlines, SCLRR can be defined as follows:

$$\min_{Z,E} \|Z\|_* + \beta |M \odot Z| + \lambda \|E\|_{2,1} \text{ s.t. } X = XZ + E, \tag{4}$$

where $\odot$ is called Hadamard product [38], β and λ are two parameters to balance the devotions of three parts. If two matrices A, B both have same size m × n, the Hadamard product means that:

$$A \odot B = \left[\begin{bmatrix} [A]_{11}[B]_{11} & \cdots & [A]_{1n}[B]_{1n} \\ \vdots & \ddots & \vdots \\ [A]_{m1}[B]_{m1} & \cdots & [A]_{mn}[B]_{mn} \end{bmatrix} \right]. \tag{5}$$

SCLRR was proved to be a better way to draw out the subspace structures of different data sets than LRR.

3 Improved Structured Low-Rank Representation

In this section, we will present an improved structured low-rank representation algorithm (ISLRR). Moreover, an optimizing algorithm is also proposed for solving ISLRR problem.

3.1 Motivation

Based on the analysis of [34], it can be found that the structure of the solution to LRR affects the subspace segmentation results directly. We could hope that the coefficient matrices obtained by LRR would be block-diagonal, namely, the relationships between intra-subspace data samples are strong and the relationships between inter-subspace data samples are weaker.

However, LRR is insufficient to handle disjoint subspace segmentation problems. For the sake of improving the ability of LRR, it is a clear way to ameliorate the structure of its solution. The purpose of introducing structural information into the algorithm is that we can achieve the block-diagonal solution even if subspaces are disjoint. From the descriptions in Sect. 2.2, SCLRR can reveal the subspace structures of data sets more precisely than LRR, however, the difficulty of SCLRR is greatly increased because of the adjustment of the additional parameter β, and an improper value of β will decrease the performance of SCLRR sharply.

Stated thus, we expect a better algorithm without extra constraint to discover the structure information of data sets. As described in SCLRR [34], M is a weighted matrix that reflects the structural relationships between data samples and a new weighted constraint $|M \odot Z|_1$ is considered to help Z to reveal the structure information of data sets better. Different from SCLRR, we apply the weighed constraint $M \odot Z$ into the equality constraint item of LRR to form a new dictionary, so that a better low rank matrix for subspace segmentation could be obtained. Considering the noise and outliers, we define the formula of ISLRR as follows:

$$\min_{Z,E} \|Z\|_* + \lambda \|E\|_{2,1} \text{ s.t. } X = X(M \odot Z) + E, \tag{6}$$

It is obvious that if we set all the elements of M as 1, we can get LRR from ISLRR. Hence, LRR is actually a special case of LRR. After Z is obtained, we define the affinity matrix as $G = (Z + Z^T)/2$ and then compute the segmentation results by Ncut [22].

In general, the property of preferable weight matrix M is that the dissimilarities between samples from intra-class are smaller and dissimilarities between interclass samples are larger. An ideal M [34] can be defined as:

$$[M]_{ij} = 1 - \exp\left(-\frac{1 - \left|x_i^{*T} x_j^*\right|}{\sigma}\right), \tag{7}$$

where x_i^* and x_j^* are the normalized data points of x_i and x_j respectively, and σ is set as the mean of $1 - \left|x_i^{*T} x_j^*\right|$ for all pairwise x_i^* and x_j^* empirically in this paper.

3.2 Optimization

In order to solve the optimization of problem (6), we introduce two auxiliary variable J and T into the objective function. Then (6) can be represented as the following equivalent form:

$$\min_{Z,E,J,T} \|J\|_* + \lambda \|E\|_{2,1} \text{ s.t. } X = XT + E, \quad Z = J, M \odot Z = T. \tag{8}$$

The augmented Lagrangian function of (8) is:

$$\mathcal{L}(Z, J, T, E, Y_a, Y_b, Y_c) = \|J\|_* + \lambda \|E\|_{2,1} + \langle Y_a, X - XT - E \rangle + \langle Y_b, Z - J \rangle$$
$$+ \langle Y_c, M \odot Z - T \rangle + \frac{\mu}{2}\left(\|X - XT - E\|_F^2 + \|Z - J\|_F^2 + \|M \odot Z - T\|_F^2\right), \tag{9}$$

where Y_a, Y_b and Y_c are Lagrange multipliers and $\mu > 0$ is a parameter. We can use an iterative approach to optimize the above unknown variables.

3.2.1 Update J with Other Variables Fixed

Suppose J^t and other variables have been obtained in the t-th iteration, ignore the irrelevent terms of J in Eq. (9), we have:

$$J^{t+1} = argmin_{J^t} \|J^t\|_* + \langle Y_b^t, Z^t - J^t \rangle + \frac{\mu^t}{2}\|Z^t - J^t\|_F^2$$
$$= argmin_{J^t} \frac{1}{\mu^t}\|J^t\|_* + \frac{1}{2}\left\|J^t - \left(Z^t + \frac{Y_b^t}{\mu^t}\right)\right\|_F^2 \tag{10}$$

then $J^{t+1} = U^t \Theta_{\frac{1}{\mu^t}}(S^t) V_t^T$, where $U^t S^t V_t^T$ is the SVD of matrix $Z^t + \frac{Y_b^t}{\mu^t}$ and Θ is a singular value thresholding operator [39].

3.2.2 Update T with Other Variables Fixed

Similar to the above method, we drop irrelevant items of T, then we have:

$$T^{t+1} = argmin_{T^t} \langle Y_a^t, X - XT^t - E^t \rangle + \langle Y_c^t, M \odot Z^t - T^t \rangle$$
$$+ \frac{\mu^t}{2}\left(\|X - XT^t - E^t\|_F^2 + \|M \odot Z^t - T^t\|_F^2\right)$$
$$= argmin_{T^t} \frac{1}{2}\left(\left\|X - XT^t - E^t + \frac{Y_a^t}{\mu^t}\right\|_F^2 + \left\|M \odot Z^t - T^t + \frac{Y_c^t}{\mu^t}\right\|_F^2\right) \tag{11}$$

then $T^{t+1} = \left(X^T X + I_n \right)^{-1} \left(X^T \left(X - E^t + \frac{Y_a^t}{\mu^t} \right) + \left(M \odot Z^t + \frac{Y_c^t}{\mu^t} \right) \right)$. I_n is an $n \times n$ identity matrix.

3.2.3 Update Z with Other Fixed Variables

Based on the above computed J^{t+1} and T^{t+1}, in the t-th iteration, we have

$$
\begin{aligned}
Z^{t+1} &= argmin_{Z^t} < Y_b^t, Z^t - J^{t+1} > + < Y_c^t, M \odot Z^t - T^{t+1} > \\
&\quad + \frac{\mu^t}{2} \left(\left\| Z^t - J^{t+1} \right\|_F^2 + \left\| M \odot Z^t - T^{t+1} \right\|_F^2 \right) \\
&= argmin_{Z^t} \frac{1}{2} \left(\left\| Z^t - J^{t+1} + \frac{Y_b^t}{\mu^t} \right\|_F^2 + \left\| M \odot Z^t - T^{t+1} + \frac{Y_c^t}{\mu^t} \right\|_F^2 \right),
\end{aligned} \tag{12}
$$

then $Z^{t+1} = \left(J^{t+1} - \frac{Y_b^t}{\mu^t} + T^{t+1} - \frac{Y_c^t}{\mu^t} \right)./(EE + M)$, where EE is an $n \times n$ matrix with each element equals 1. Suppose $C = A./B$, then $[C]_{ij} = [A]_{ij}/[B]_{ij}$.

3.2.4 Update *E* with Other Fixed Variables

Abandon the irrelevant terms in (9) w.r.t E, then we could have:

$$
\begin{aligned}
E^{t+1} &= argmin_{E^t} \lambda \| E^t \|_{2,1} + < Y_a^t, X - XT^{t+1} - E^t > + \frac{\mu^t}{2} \left\| X - XT^{t+1} - E^t \right\|_F^2 \\
&= argmin_{E^t} \frac{\lambda}{\mu} \| E^t \|_{2,1} + \frac{1}{2} \left\| X - XT^t - E^t + \frac{Y_a^t}{\mu^t} \right\|_F^2,
\end{aligned} \tag{13}
$$

Finally, the update schemes of for the Lagrange multipliers Y_a, Y_b and Y_c and parameter μ are summarized as follows:

$$
\begin{aligned}
Y_a^{t+1} &= Y_a^t + \mu^t \left(X - XT^{t+1} - E^{t+1} \right), \\
Y_b^{t+1} &= Y_b^t + \mu^t \left(Z^{t+1} - J^{t+1} \right), \\
Y_c^{t+1} &= Y_c^t + \mu^t \left(M \odot Z^{t+1} - T^{t+1} \right), \\
\mu^{t+1} &= \min \left(\mu_{max}, \rho \mu^t \right),
\end{aligned} \tag{14}
$$

where μ_{max} and ρ are two adjustable parameters.

3.3 Algorithm

According to the descriptions above, ISLRR algorithm can be summarized as follows

---

Algorithm 1 Improved Structured Low-Rank Representation (ISLRR)

Input: A data set $X = [x_1, x_2, \cdots, x_n]$, the parameter λ, the weighted matrix M, and the maximal number of iteration Maxiter.

Output: The coefficient matrix T, the low rank matrix Z and the noise matrix E.

1. Initialize the variables and parameters:
$Y_a^0 = Y_b^t = Y_c^t = 0, \mu^0 = 10^{-6}, \mu_{max} = 10^{10}, \rho = 1.1, \varepsilon = 10^{-8}, t = 0, Z^0 = J^0 = T^0 = 0,$

2. **While** $\|X - XT^t - E^t\|_F^2 > \varepsilon$, $\|Z^t - J^t\|_F^2 > \varepsilon$, $\|M \odot Z^t - T^t\|_F^2 > \varepsilon$ and $t <$ Maxiter

3. Update $J^{t+1}, T^{t+1}, Z^{t+1}, E^{t+1}$ by solving Eq. (10) to Eq. (13);

4. Update $Y_a^{t+1}, Y_b^{t+1}, Y_c^{t+1}, \mu^{t+1}$ by solving Eq.(14) ;

5. $t = t + 1$;

6. **end while**

7. **return:** the matrix $T^* = T^t$, the low rank matrix $Z^* = Z^t$, the noise matrix $E^* = E^t$,

---

4 Further Discussion

4.1 The Relationship Between SCLRR and ISLRR

Comparing SCLRR with our ISLRR, it can be found that:

1. In order to improve the applications of LRR on data sets with disjoint subspaces, both SCLRR and ISLRR introduce the weighted matrix M to the coefficient matrix Z for enhancing its structure information, as is to say, they both have the same weighted coefficient matrix M ⊙ Z.

2. In this article, the way to define the weighted matrix M is same as that used in [34], namely $[M]_{ij} = 1 - \exp\left(-\frac{1-\left|x_i^{*T} x_j^*\right|}{\sigma}\right)$. In the future works, we can also take more appropriate ways to get a better M.

3. According to Eq. (4), SCLRR introduces the weighted matrix $M \odot Z = \sum_{i,j} M_{ij} |Z|_{i,j}$ as the sparse constraint item into the objective function of LRR for balancing the nuclear norm to get a better low rank solution. But ISLRR treats the weighed matrix $M \odot Z = \sum_{i,j} M_{ij} |Z|_{i,j}$ as a new dictionary for representing data samples more accurately. Therefore, we can also get a more suitable structural low rank matrix for subspace segmentation.

4.2 Algorithm Convergence

In Sect. 3.2, ISLRR uses ADM to get the optimum solution, whose convergence has been validated when the number of variables is less than or equal to two [40]. Since there are four variables: Z, J, T and E in Algorithm 1, it is difficult to give the theoretical explanation to illustrate the convergence of algorithm. Fortunately, Eckstein et al. [41] provided two sufficient conditions to guarantee the convergence of the algorithms: one is that the dictionary matrix in the equality constraints should be of full column rank; the other is that the optimal solution of each variable is monotonically decreasing in each iteration step. According to [41], the dataset Z is a full column rank matrix, since the row elements of the weight matrix M are not all zero, it is easy to verify that the dictionary matrix M ⊙ Z is of full column rank. However, the monotonically decreasing condition cannot be proved directly, while
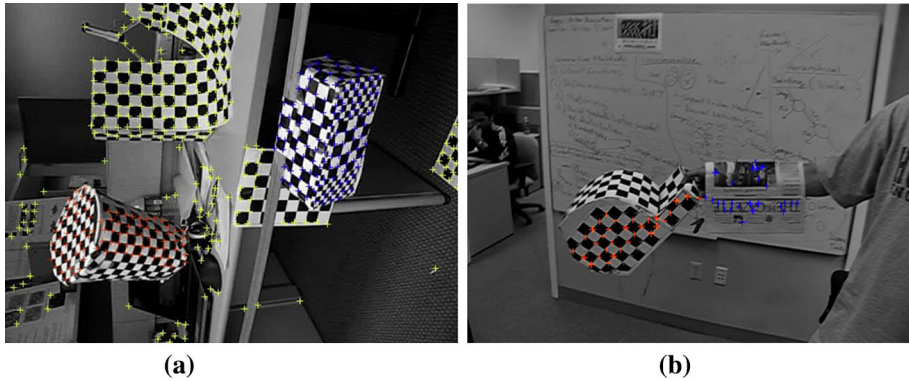
Fig. 2 Sample images of Hopkins 155 motion database. **a** 1R2RC, **b** arm

the convexity of Lagrange's function ensures its effectiveness to a certain extent [41]. In a word, we expect Algorithm 1 to be convergent and use the upper bounded μ to guarantee its theoretical convergence in the alternating direction method, but its strict proof of convergence is worth further discussion.

5 Experiments

In this section, we evaluate the performance of ISLRR for subspace segmentation problems. The close related algorithms including SSC [15], LRR [7, 18], and SCLRR [34] are used for comparisons. The frequently used databases such as Hopkins 155 [42], Fashion_MNIST [37], two face image databases Extended Yale B [43] and AR [44] are used in our experiments.

The computer configurations for these experiments are 3.20 GHz Inter (R) Core (TM) i5-6500 CPU with 4 GB machine memory, 500G hard disk memory, 64 bit windows7 professional operating system, and R2014a version Matlab.

These four databases are described briefly as follows:

Hopkins 155 motion segmentation data set contains 155 sequences, which includes 104 checkerboard sequences, 38 traffic sequences, and 13 others. Each of sequence is an independent clustering task, so there are altogether 156 clustering tasks. The sample images from Hopkins 155 database are given in Fig. 2.

Fashion-MNIST data set consists of 60,000 train examples and 10,000 test examples. They are divided into 10 categories: t-shirt, trouser, pullover, dress, coat, sandal, shirt, sneaker, bag, and ankle boo. We select the first 50 pictures of each class' train data set, and resize them to 20×20 pixels in our experiments. The samples are given in Fig. 3a.

Extended Yale B face database consists of 38 objects with a total of 2414 images, each of which has 9 different gestures with 64 Gray scales. Moreover, these photos were taken in different light and facial expressions. In our experiment, each picture is resized to 32×32 pixels. The samples are given in Fig. 3b.

AR face database contains more than 4000 face images of 126 objects. Each object has 26 pictures in two modes, therefore each mode has 13 pictures. These images are taken in different views and lights. In our experiment, we select altogether 2000 photos from the first 120 people and adjust each image to 50×40 pixels. The image samples are shown in Fig. 3c.
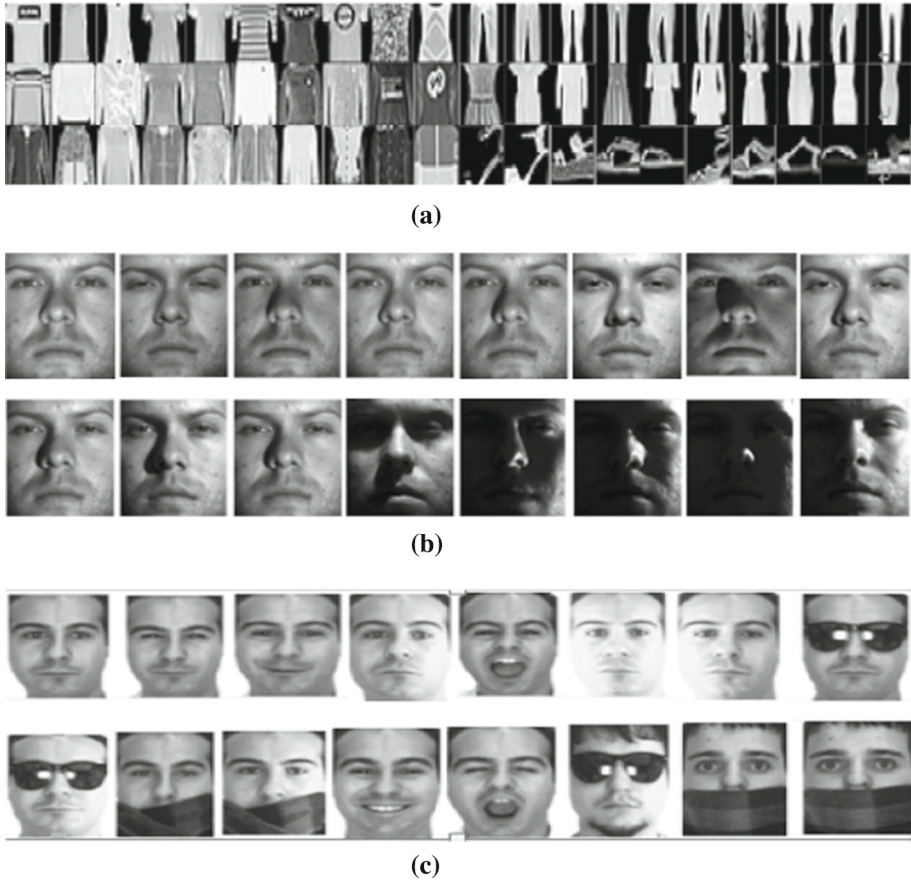
(a)

(b)

(c)

Fig. 3 Static sample images from three image databases. **a** Sample images of Fashion-MNIST database, **b** sample images of the extend Yale B database and **c** sample images of AR database

5.1 Comparisons with LRR

In this subsection, we carry the experiments on three static image data sets to observe the relationship between LRR and ISLRR. The first four categories of each data set are selected for this experiment and parameter λ in both algorithms are set to 1. In Fig. 4, Z_{LRR} is the low rank coefficient matrix of LRR, Z_{ISLRR} is the low rank constraint matrix of ISLRR. M is the structural features matrix of data samples.

From Fig. 4, we can see that: (1) Z_{ISLRR} is a dialog matrix, as is to say, Z_{ISLRR} can be a better matrix to design an affinity graph for subspace segmentation; (2) the low rank matrix Z_{ISLRR} is different from Z_{LRR} of LRR, and it is also not equal to $Z_{LRR}./M$. This means that Z_{ISLRR} could not be directly computed as $Z_{LRR}./M$. Therefore, it is reliable to introduce the structure information of data sets into LRR by following the methodology of ISLRR.

Z_{LRR}

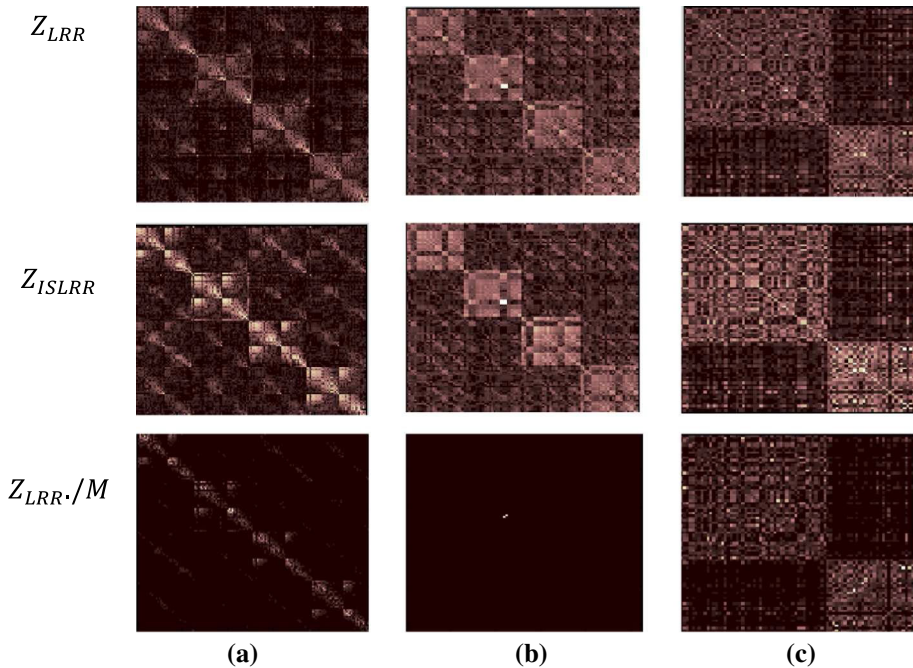Z_{ISLRR}

$Z_{LRR}./M$

(a)   (b)   (c)

Fig. 4 The reconstruction coefficient matrices obtained by LRR and SLRR. **a** Extend Yale B, **b** AR and **c** Fashion-MINST

5.2 Sensitivity Analysis

In the first section, we took a simple test to observe the sensitivity of SCLRR to the extra parameter β and claimed that the performance of SCLRR varies drastically with β. In this section, a series of experiments are conducted to observe the sensitivity of ISLRR and SCLRR to the corresponding parameters. For Hopkins 155, we choose 1R2RC sequence for this experiment, and the range of parameter β is set as [0.001, 50] while λ is chosen in [0.0001, 20]. For the three static image databases, we select the first three classes of each dataset and set the intervals of λ and β as [0.001, 50]. In the experiments on SCLRR, we fix one parameter at their corresponding optimal point to observe the accuracy along with the change of another parameter. The experiments results are shown in Fig. 5.

From Fig. 5, we can find that: (1) parameter β will affect the final results of SCLRR directly even if the parameter λ is fixed in the corresponding optimal value; (2) in most cases, the sensitivity of ISLRR to the parameter λ is similar to that of SCLRR when β is fixed in its optimal value. But in general, it is much easier to adjust one parameter in ISLRR than to adjust two in SCLRR.

5.3 Comparisons with Related Algorithms

To further verify the effectiveness of ISLRR, ISLRR and other related algorithms are evaluated on the four databases for comparisons.
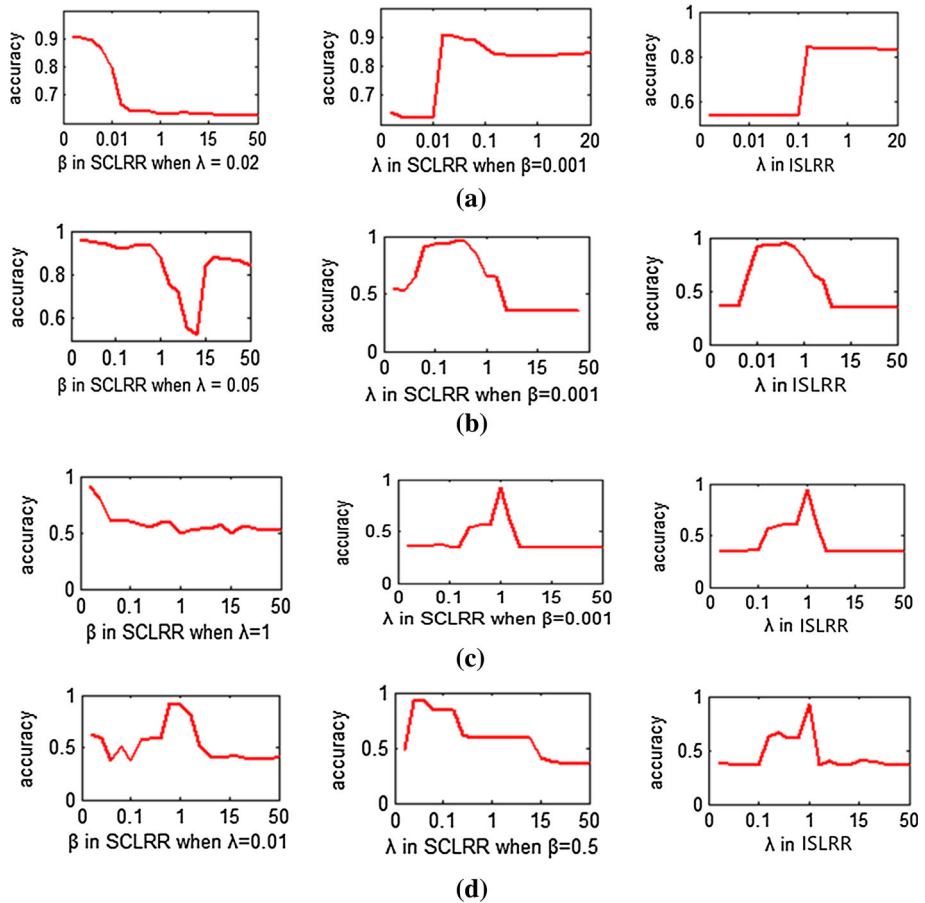
Fig. 5 The performaces of SCLRR and ISLRR varied with the corresponding parameters. **a** 1R2RC, **b** the Extended Yale B, **c** AR and **d** Fashion-MINIST

5.3.1 Experiments on Motion Sequences

For Hopkins 155 data set, these motion sequences can be regarded as different categories, so we can consider such problems as 120 two-class segmentation problems and 35 three-class segmentation problems. The segmentation results of related algorithms including mean values (Ave.), standard deviations (Std.), and maxima errors (Max.) are reported in Table 1 (The optimal values of different criteria are emphasized in bold).

From the Table 1, we can see that ISLRR achieved better results in two motion sequences than those in three motion sequences. Compared with the related algorithms, ISLRR can reach more promising results.

5.3.2 Experiments on Static Image Datasets

In this subsection, we first find the highest accuracies of the four algorithms with the corresponding optimal parameters on three static image databases, and record the running times of

Table 1 Segmentation error (%) of different algorithms on Hopkins 155 data set

	2 motions			3 motions			Total		
	Ave.	Std.	Max.	Ave.	Std.	Max	Ave.	Std.	Max.
SSC	4.65	10.11	48.62	8.19	10.23	42.93	5.45	10.21	48.62
LRR	4.33	9.82	48.61	**8.15**	**10.23**	**38.30**	5.20	10.01	48.61
SCLRR	3.74	8.56	**47.22**	9.45	11.20	40.43	5.03	**9.49**	**47.22**
ISLRR	**3.72**	**9.74**	48.82	9.30	10.54	40.26	**4.98**	9.92	48.82

SSC $\lambda = 1$, *LLR* $\lambda = 2.4$, *SCLRR* $\beta = 0.01$, $\lambda = 2$, *ISLRR* $\lambda = 4$

Table 2 The experiment results of different algorithms on three image data sets

	SSC	LRR	SCLRR	ISLRR
The extend Yale B (%)	0.6031	0.6333	0.6675	**0.6831**
Parameters	$\lambda = 0.5$	$\lambda = 3$	$\beta = 0.001, \lambda = 3$	$\lambda = 3.5$
Running times (s)	590.46	2421.94	3131.67	3122.04
AR (%)	0.6651	0.7808	0.7885	**0.7975**
Parameters	$\lambda = 0.5$	$\lambda = 1$	$\beta = 3, \lambda = 1$	$\lambda = 3$
Running times (s)	1205.03	2144.15	3072.88	2478.11
Fashion-MNIST (%)	0.5360	0.5660	0.5600	**0.5760**
Parameters	$\lambda = 0.5$	$\lambda = 0.4$	$\beta = 0.1, \lambda = 0.35$	$\lambda = 0.1$
Running times (s)	9.38	13.50	21.55	16.38

each algorithm in each database. The experimental results are shown in Table 2 (The optimal values of different criteria are emphasized in bold).

From Table 2, we see that: (1) ISLRR and SCLRR spend more time on three image data sets for better results; (2) ISLRR can obtain the highest segmentation accuracies on all the three databases.

Next, we compare the performances of related algorithms on each data set with different number of classes. In those experiments, we choose q (q is between 3 and the total number classes of data samples) classes data samples to compute their corresponding accuracies. The range of parameter λ is set as [0.001, 20] and parameter β is [0.0001, 50], and the best results are recorded in Fig. 6.

From Fig. 6, we can see that: (1) with the increment of segmentation data categories, the segmentation accuracies of these algorithms decline; (2) ISLRR is superior to other algorithms in most cases, especially on Yale B data set. The experimental results show that ISLRR is an effective algorithm in dealing with the segmentation problems of static images.

6 Conclusions

In this paper, a new subspace segmentation algorithm named ISLRR is proposed. In ISLRR, we introduce the structure information of data sets into the equality constraint term of LRR. Comparing with SCLRR, it doesn't bring any extra parameter, thus it avoids the difficulty for adjusting two parameters. To confirm the algorithm's effectiveness, three close related
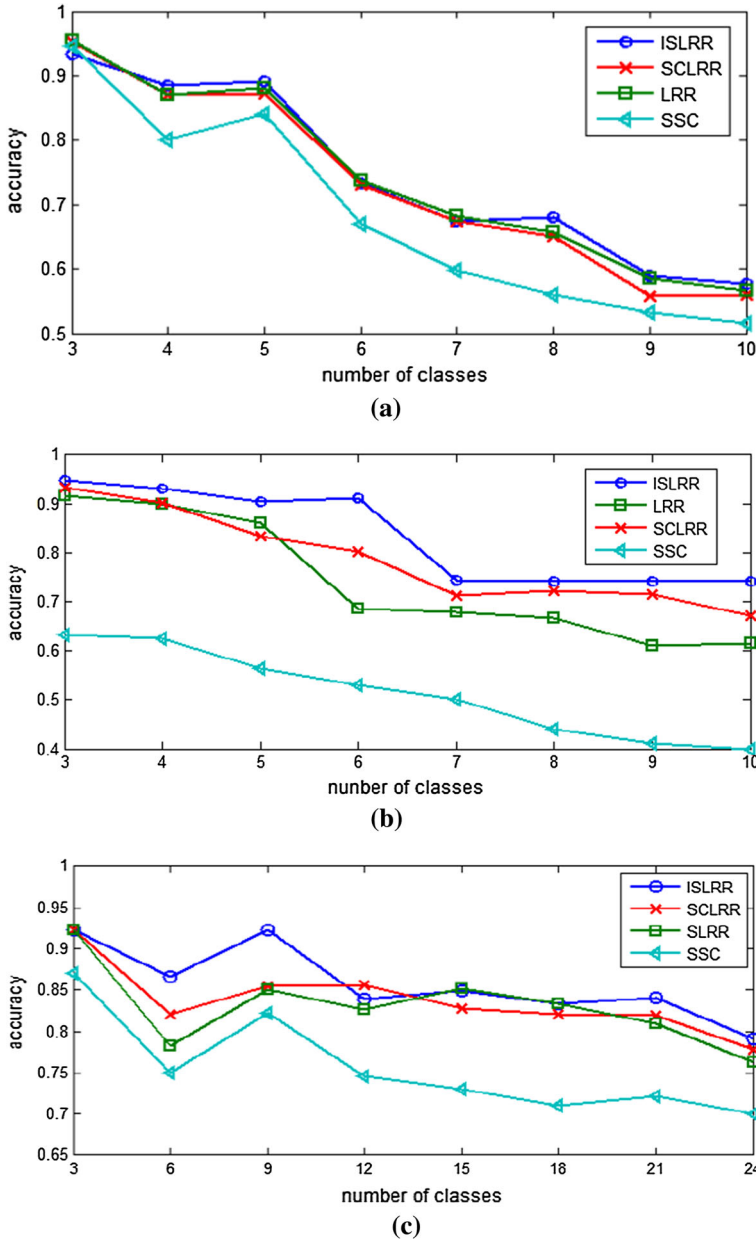
Fig. 6 The segmentation accuracies obtained by evaluated algorithms versus the number of classes on different databases. **a** Experimental results on Fashion-MINIST database, **b** experimental results on the Extended Yale B database and **c** experimental results on AR database

algorithms are also evaluated on four image data sets. Experimental results show that ISLRR algorithm is simply and effective for handling subspace segmentation problems.

Compliance with Ethical Standards

Conflict of interest The authors declared that we have no financial and personal relationships with other people or organizations that can inappropriately influence our work, there is no professional or other personal interest of any nature or kind in any product, service and/or company that could be construed as influencing the position presented in, or the review of, the manuscript entitled.

References

1. Hong W, Wright J, Huang K, Ma Y (2006) Multi-scale hybrid linear models for lossy image representation. IEEE Trans Image Process 15(12):3655–3671
2. Costeira J, Kanade T (1998) A multibody factorization method for independently moving objects. Int J Comput Vis 29(3):159–179
3. Kanatani K (2001) Motion segmentation by subspace separation and model selection. In: IEEE international conference on computer vision, vol 2, pp 586–591
4. Yan J, Pollefeys M (2006) A general framework for motion segmentation: independent, articulated, rigid, non-rigid, degenerate and nondegenerate. In: European Conference on Computer Vision, pp 94–106
5. Zelnik-Manor L, Irani M (2003) Degeneracies, dependencies and their implications in multi-body and multi-sequence factorization. In: IEEE conference on computer vision and pattern recognition, vol 2, pp 287–293
6. Vidal R, Favaro P (2014) Low rank subspace clustering. Pattern Recognit Lett 43:47–61
7. Liu G, Lin Z, Yan S, Sun J, Yu Y, Ma Y (2013) Robust recovery of subspace structures by low-rank representation. IEEE Trans Pattern Anal Mach Intell 35:171–184
8. Wei L, Wang X, Yin J, Wu A (2016) Spectral clustering steered low-rank representation for subspace segmentation]. J Vis Commun Image Represent 38:386–395
9. Huang K, Ma Y, Vidal R (2004) Minimum effective dimension for mixtures of subspaces: a robust GPCA algorithm and its applications. In: IEEE conference on computer vision and pattern recognition (CVPR), pp 631–638
10. Ma Y, Yang AY, Derksen H, Fossum R (2008) Estimation of subspace arrangements with applications in modeling and segmenting mixed data. SIAM Rev 50(3):413–458
11. Zhang T, Szlam A, Wang Y, Lerman G (2012) Hybrid linear modeling via local bestfit flats. Int J Comput Vis 100(3):217–240
12. Bradley PS, Mangasarian OL (2000) K-plane clustering. J Glob Optim 16(1):23–32
13. Leonardis A, Bischof H, Maver J (2002) Multiple eigenspaces. Pattern Recogn 35(11):2613–2627
14. Ma Y, Derksen H, Hong W, Wright J (2007) Segmentation of multivariate mixed data via lossy coding and compression. IEEE Trans Pattern Anal Mach Intell 29(9):1546–1562
15. Elhamifar E, Vidal R (2009) Sparse subspace clustering. In: CVPR
16. Patel VM, Nguyen HV, Vidal R (2013) Latent space sparse subspace clustering. In: ICCV, pp 225–232
17. Lu C, Tang J, Lin M, Lin L, Yan S, Lin Z (2013) Correntropy induced L2 graph for robust subspace clustering. In: ICCV, pp 1801–1808
18. Liu G, Lin Z, Yu Y (2010) Robust subspace segmentation by low-rank representation. In: ICML-10, Haifa, Israel, pp 663–670
19. Wei L, Wu A, Yin J (2015) Latent space robust subspace segmentation based on low rank and locality constraints. Expert Syst Appl 42:6598–6608
20. Elhamifar E, Vidal R (2013) Sparse subspace clustering: algorithm, theory, and applications. IEEE Trans Pattern Anal Mach Intell 35(11):2765–2781
21. Wei L, Wang X, Yin J, Wu A (2017) Self-regularized fixed-rank representation for subspace segmentation. Inf Sci 412–413:194–209
22. Shi J, Malik J (2000) Normalized cuts and image segmentation. IEEE Trans Pattern Anal Mach Intell 22:888–905
23. Wright J, Yang A, Ganesh A, Sastry SS, Ma Y (2009) Robust face recognition via sparse representation. IEEE Trans Pattern Anal Mach Intell 31(2):210–227
24. Wang Y, Xu C, You S, Xu C, Tao D (2017) DCT regularized extreme visual recovery. IEEE Trans Image Process 26(7):3360–3371

25. Liu Q, Lai Z, Zhou Z, Kuang F, Jin Z (2015) A truncated nuclear norm regularization method based on weighted residual error for matrix completion. IEEE Trans Image Process 25(1):316–330
26. Wang Y, Xu C, Xu C, Tao D (2017) Beyond RPCA: flattening complex noise in the frequency domain In: AAAI conference on artificial intelligence
27. Hu Y, Zhang D, Ye J, Li X, He X (2013) Fast and accurate matrix completion via truncated nuclear norm regularization. IEEE Trans Pattern Anal Mach Intell 35(9):2117–2130
28. Li J, Xu C, Yang W, Sun C, Tao D (2017) Discriminative multi-view interactive image re-ranking. IEEE Trans Image Process 26(7):3113–3127
29. Li J, Xu C, Yang W, Sun C (2017) SPA: spatially pooled attributes for image retrieval. Neurocomputing 257:47–58
30. Chen J, Zhang H, Mao H, Sang Y, Yi Z (2014) Symmetric low-rank representation for subspace clustering. Neurocomputing 173(3):1192–1202
31. Zhuang L, Wang J, Lin Z, Yang AY, Ma Y, Yu N (2016) Locality-preserving low-rank representation for graph construction from nonlinear manifolds. Neurocomputing 175:715–722
32. Zhang YL, Jiang Z, Larry S (2013) Learning structured low-rank representations for image classification. In: Computer vision and pattern recognition, pp 676–683
33. Zhuang L, Gao H, Lin Z, Ma Y, Zhang X, Yu N (2012) Non-negative low rank and sparse graph for semi-supervised learning, In: CVPR, pp 2328–2335
34. Tang K, Liu R, Su Z, Zhang J (2014) Structure-constrained low-rank representation. IEEE Trans Neural Netw Learn Syst 25(12):2167–2179
35. Li X, Li X, Liu C, Liu H (2016) Structure-constrained low-rank and partial sparse representation with sample selection for image classification. Pattern Recognit 59:5–13
36. Wu T, Gurram P, Rao RM, Bajwa W (2016) Clustering-aware structure-constrained low-rank representation model for learning human action attributes. In: Image, video, and multidimensional signal processing workshop. IEEE, pp 1–5
37. Xiao H, Rasul K, Vollgraf R (2017) Fashion-MNIST: a novel image dataset for benchmarking machine learning algorithms. arXiv:1708.07747
38. Zhang X (2004) Matrix analysis and applications. Springer, New York
39. Cai JF, Candès EJ, Shen Z (2008) A singular value thresholding algorithm for matrix completion. SIAM J Optim 20(4):1956–1982
40. Lin Z, Chen M, Wu L, Ma Y (2009) The augmented Lagrange multiplier method for exact recovery of corrupted low-rank matrices. In: UIUC, Champaign, IL, USA, Technical Report UILU-ENG-09-2215
41. Eckstein J, Bertsekas DP (1992) On the Douglas-Rachford splitting method and the proximal point algorithm for maximal monotone operators. Math Program 55(1–3):293–318
42. Tron R, Vidal R (2007) A benchmark for the comparison of 3-D motion segmentation algorithms. In: IEEE international conference on computer vision and pattern recognition (ICCV)
43. Samaria F, Harter A (1994) Parameterisation of a stochastic model for human face identification. In: Proceedings of 2nd IEEE workshop applications of computer vision
44. Lee KC, Ho J, Driegman D (2005) Acquiring linear subspaces for face recognition under variable lighting. IEEE Trans Pattern Anal Mach Intell 27(5):684–698